11. Fluid Jets

11.1   The shape of a falling fluid jet

Consider a circular orifice of a radius a ejecting a flux Q of fluid density ρ and kinematic viscosity ν (see Fig. 11.1). The resulting jet accelerates under the influence of gravity $-g\hat{z}$. We assume that the jet Reynolds number $\mathcal{Re} = Q/(a\nu)$ is sufficiently high that the influence of viscosity is negligible; furthermore, we assume that the jet speed is independent of radius, and so adequately described by $U(z)$. We proceed by deducing the shape $r(z)$ and speed $U(z)$ of the evolving jet.

Applying Bernoulli's Theorem at points A and B:

$$\frac{1}{2}\rho U_0^2 + \rho g z + P_A = \frac{1}{2}\rho U^2(z) + P_B \tag{11.1}$$

The local curvature of slender threads may be expressed in terms of the two principal radii of curvature, R_1 and R_2:

$$\boldsymbol{\nabla} \cdot \boldsymbol{n} = \frac{1}{R_1} + \frac{1}{R_2} \approx \frac{1}{r} \tag{11.2}$$

Thus, the fluid pressures within the jet at points A and B may be simply related to that of the ambient, P_0:

$$P_A \approx P_0 + \frac{\sigma}{a} \quad , \quad P_B \approx P_0 + \frac{\sigma}{r} \tag{11.3}$$

Substituting into (11.1) thus yields

$$\frac{1}{2}\rho U_0^2 + \rho g z + P_0 + \frac{\sigma}{a} = \frac{1}{2}\rho U^2(z) + P_0 + \frac{\sigma}{r} \tag{11.4}$$

from which one finds

$$\frac{U(z)}{U_0} = \left[1 + \underbrace{\frac{2}{\mathcal{F}r}\frac{z}{a}}_{\text{acc. due to } g} + \underbrace{\frac{2}{\mathcal{W}e}\left(1 - \frac{a}{r}\right)}_{\text{dec. due to } \sigma} \right]^{1/2} \tag{11.5}$$

where we define the dimensionless groups

$$\mathcal{F}r = \frac{U_0^2}{ga} = \frac{INERTIA}{GRAVITY} = Froude\ Number \tag{11.6}$$

$$\mathcal{W}e = \frac{\rho U_0^2 a}{\sigma} = \frac{INERTIA}{CURVATURE} = Weber\ Number \tag{11.7}$$

Now flux conservation requires that

$$Q = 2\pi \int_0^r U(z) r(z) dr = \pi a^2 U_0 = \pi r^2 U(z) \tag{11.8}$$

from which one obtains

$$\frac{r(z)}{a} = \left(\frac{U_0}{U(z)}\right)^{1/2} = \left[1 + \frac{2}{\mathcal{F}r}\frac{z}{a} + \frac{2}{\mathcal{W}e}\left(1 - \frac{a}{r}\right)\right]^{-1/4} \tag{11.9}$$

This may be solved algebraically to yield the thread shape $r(z)/a$, then this result substituted into (11.5) to deduce the velocity profile $U(z)$. In the limit of $\mathcal{W}e \to \infty$, one obtains

$$\frac{r}{a} = \left(1 + \frac{2gz}{U_0^2}\right)^{-1/4}, \ \frac{U(z)}{U_0} = \left(1 + \frac{2gz}{U_0^2}\right)^{1/2} \tag{11.10}$$
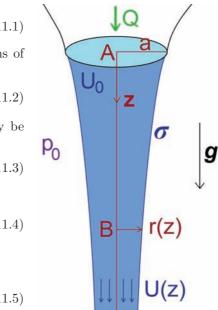

Figure 11.1: A fluid jet extruded from an orifice of radius a accelerates under the influence of gravity. Its shape is influenced both by the gravitational acceleration $\boldsymbol{g}$ and the surface tension σ. Note that σ gives rise to a gradient in curvature pressure within the jet, $\sigma/r(z)$, that opposes the acceleration due to $\boldsymbol{g}$.

11.2   The Plateau-Rayleigh Instability

We here summarize the work of Plateau and Rayleigh on the instability of cylindrical fluid jets bound by surface tension. It is precisely this Rayleigh-Plateau instability that is responsible for the pinch-off of thin water jets emerging from kitchen taps (see Fig. 11.2).

The equilibrium base state consists of an infinitely long quiescent cylindrical inviscid fluid column of radius R_0, density ρ and surface tension σ (see Fig. 11.3). The influence of gravity is neglected. The pressure p_0 is constant inside the column and may be calculated by balancing the normal stresses with surface tension at the boundary. Assuming zero external pressure yields

$$p_0 = \sigma \boldsymbol{\nabla} \cdot \boldsymbol{n} \Rightarrow p_0 = \frac{\sigma}{R_0} \ . \tag{11.11}$$

We consider the evolution of infinitesimal varicose perturbations on the interface, which enables us to linearize the governing equations. The perturbed columnar surface takes the form:

$$\tilde{R} = R_0 + \epsilon e^{\omega t + ikz} \quad , \tag{11.12}$$

where the perturbation amplitude $\epsilon \ll R_0$, ω is the growth rate of the instability and k is the wave number of the disturbance in the z-direction. The corresponding wavelength of the varicose perturbations is necessarily $2\pi/k$. We denote by $\tilde{u}_r$ the radial component of the perturbation velocity, $\tilde{u}_y$ the axial component, and $\tilde{p}$ the perturbation pressure. Substituing these perturbation fields into the N-S equations and retaining terms only to order ϵ yields:

$$\frac{\partial \tilde{u}_r}{\partial t} = -\frac{1}{\rho} \frac{\partial \tilde{p}}{\partial r} \tag{11.13}$$

$$\frac{\partial \tilde{u}_z}{\partial t} = -\frac{1}{\rho} \frac{\partial \tilde{p}}{\partial z} \tag{11.14}$$

The linearized continuity equation becomes:

$$\frac{\partial \tilde{u}_r}{\partial r} + \frac{\tilde{u}_r}{r} + \frac{\partial \tilde{u}_z}{\partial z} = 0 \ . \tag{11.15}$$

We anticipate that the disturbances in velocity and pressure will have the same form as the surface disturbance (11.12), and so write the perturbation velocities and pressure as:

$$(\tilde{u}_r, \tilde{u}_z, \tilde{p}) = \Big(R(r), Z(r), P(r)\Big) e^{\omega t + ikz} \ . \tag{11.16}$$

Substituting (11.16) into equations (11.13-11.15) yields the linearized equations governing the perturbation fields:

$$\text{Momentum equations :} \quad \omega R = -\frac{1}{\rho} \frac{dP}{dr} \tag{11.17}$$

$$\omega Z = -\frac{ik}{\rho} P \tag{11.18}$$

$$\text{Continuity:} \quad \frac{dR}{dr} + \frac{R}{r} + ikZ = 0 \ . \tag{11.19}$$

Figure 11.2: The capillary-driven instability of a water thread falling under the influence of gravity. The initial jet diameter is approximately 3 mm.
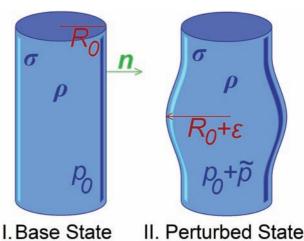

I. Base State   II. Perturbed State

Figure 11.3: A cylindrical column of initial radius R_0 comprised of an inviscid fluid of density ρ, bound by surface tension σ.

Eliminating $Z(r)$ and $P(r)$ yields a differential equation for $R(r)$:

$$r^2 \frac{d^2R}{dr^2} + r\frac{dR}{dr} - \left(1 + (kr)^2\right)R = 0 \quad . \tag{11.20}$$

This corresponds to the modified Bessel Equation of order 1, whose solutions may be written in terms of the modified Bessel functions of the first and second kind, respectively, $I_1(kr)$ and $K_1(kr)$. We note that $K_1(kr) \to \infty$ as $r \to 0$; therefore, the well-behavedness of our solution requires that $R(r)$ take the form

$$R(r) = CI_1(kr) \quad , \tag{11.21}$$

where C is an as yet unspecified constant to be determined later by application of appropriate boundary conditions. The pressure may be obtained from (11.21) and (11.17), and by using the Bessel function identity $I'_0(\xi) = I_1(\xi)$:

$$P(r) = -\frac{\omega\rho C}{k}I_0(kr) \quad \text{and} \quad Z(r) = -\frac{ik}{\omega\rho}P(r). \tag{11.22}$$

We proceed by applying appropriate boundary conditions. The first is the kinematic condition on the free surface:

$$\frac{\partial \tilde{R}}{\partial t} = \tilde{\boldsymbol{u}} \cdot \boldsymbol{n} \approx \tilde{u}_r \quad . \tag{11.23}$$

Substitution of (11.21) into this condition yields

$$C = \frac{\epsilon\omega}{I_1(kR_0)} \quad . \tag{11.24}$$

Second, we require a normal stress balance on the free surface:

$$p_0 + \tilde{p} = \sigma\boldsymbol{\nabla} \cdot \boldsymbol{n} \tag{11.25}$$

We write the curvature as $\sigma\boldsymbol{\nabla} \cdot \boldsymbol{n} = \left(\frac{1}{R_1} + \frac{1}{R_2}\right)$, where R_1 and R_2 are the principal radii of curvature of the jet surface:

$$\frac{1}{R_1} = \frac{1}{R_0 + \epsilon e^{\omega t + ikz}} \approx \frac{1}{R_0} - \frac{\epsilon}{R_0^2}e^{\omega t + ikz} \tag{11.26}$$

$$\frac{1}{R_2} = \epsilon k^2 e^{\omega t + ikz} \quad . \tag{11.27}$$

Substitution of (11.26) and (11.27) into equation (11.25) yields:

$$p_0 + \tilde{p} = \frac{\sigma}{R_0} - \frac{\epsilon\sigma}{R_0^2}\left(1 - k^2R_0^2\right)e^{\omega t + ikz} \tag{11.28}$$

Cancellation via (11.11) yields the equation for $\tilde{p}$ accurate to order ϵ:

$$\tilde{p} = -\frac{\epsilon\sigma}{R_0^2}\left(1 - k^2R_0^2\right)e^{\omega t_i kz} \quad . \tag{11.29}$$

Combining (11.22), (11.24) and (11.29) yields the dispersion relation, that indicates the dependence of the growth rate ω on the wavenumber k:

$$\omega^2 = \frac{\sigma}{\rho R_0^3}kR_0\frac{I_1(kR_0)}{I_0(kR_0)}\left(1 - k^2R_0^2\right) \tag{11.30}$$

We first note that unstable modes are only possible when

$$kR_0 < 1 \tag{11.31}$$

The column is thus unstable to disturbances whose wavelengths exceed the circumference of the cylinder. A plot of the dependence of the growth rate ω on the wavenumber k for the Rayleigh-Plateau instability is shown in Fig. 11.4.

The fastest growing mode occurs for $kR_0 = 0.697$, i.e. when the wavelength of the disturbance is

$$\lambda_{max} \approx 9.02 R_0 \tag{11.32}$$

By inverting the maximum growth rate ω_{max} one may estimate the characteristic break-up time:

$$t_{breakup} \approx 2.91 \sqrt{\frac{\rho R_0^3}{\sigma}} \tag{11.33}$$

Figure 11.4: The dependence of the growth rate ω on the wavenumber k for the Rayleigh-Plateau instability.

Note: In general, pinch-off depends on $\mathcal{O}h = \frac{\mu\nu}{\sigma R}$.

At low $\mathcal{O}h$, we have seen that $\tau_{pinch} \sim \left(\frac{\rho R^2}{\sigma}\right)^{1/2}$, $\lambda = 9.02R$.

At high $\mathcal{O}h$, when viscosity is important, $\tau_{pinch} \sim \frac{\mu R}{\sigma}$, λ increases with μ.

A water jet of diameter 1cm has a characteristic break-up time of about 1/8s, which is consistent with casual observation of jet break-up in a kitchen sink.

Related Phenomena: Waves on jets

When a vertical water jet impinges on a horizontal reservoir of water, a field of standing waves may be excited on the base of the jet (see Fig. 11.5). The wavelength is determined by the requirement that the wave speed correspond to the local jet speed: $U = -\omega/k$. Using our dispersion relation (11.30) thus yields

$$U^2 = \frac{\omega^2}{k^2} = \frac{\sigma}{\rho k R_0^2} \frac{I_1(kR_0)}{I_0(kR_0)} \left(1 - k^2 R_0^2\right) \tag{11.34}$$
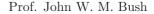
Provided the jet speed U is known, this equation may be solved in order to deduce the wavelength of the waves that will travel at U and so appear to be stationary in the lab frame. For jets falling from a nozzle, the result (11.5) may be used to deduce the local jet speed.

11.3 Fluid Pipes

The following system may be readily observed in a kitchen sink. When the volume flux exiting the tap is such that the falling stream has a diameter of $2 - 3$mm, obstructing the stream with a finger at a distance of several centimeters from the tap gives rise to a stationary field of varicose capillary waves upstream of the finger. If the finger is dipped in liquid detergent (soap) before insertion into the stream, the capillary waves begin at some critical distance above the finger, below which the stream is cylindrical. Closer inspection reveal that the surface of the jet's cylindrical base is quiescent.

An analogous phenomenon arises when a vertical fluid jet impinges on a deep water reservoir (see Fig. 11.5). When the reservoir is contaminated by surfactant, the surface tension of the reservoir is diminished relative to that of the jet. The associated surface tension gradient draws surfactant a finite distance up the jet, prompting two salient alterations in the jet surface. First, the surfactant suppresses surface waves, so that the base of the jet surface assumes a cylindrical form (Fig. 11.5b). Second, the jet surface at its base becomes stagnant: the Marangoni stresses associated with the surfactant gradient are balanced by the viscous stresses generated within the jet. The quiescence of the jet surface may be simply demonstrated by sprinkling a small amount of talc or lycopodium powder onto the jet. The fluid jet thus enters a contaminated reservoir as if through a rigid pipe.

A detailed theoretical description of the fluid pipe is given in *Hancock & Bush (JFM, 466, 285-304)*. We here present a simple scaling that yields the dependence of the vertical extent H of the fluid pipe on
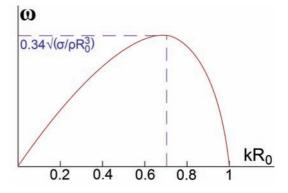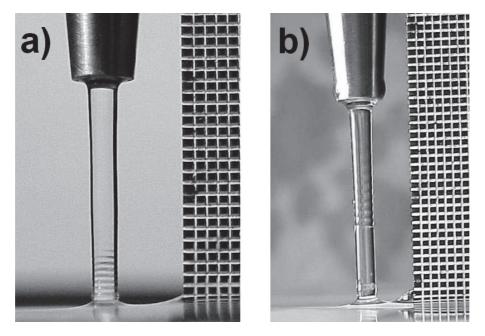
Figure 11.5: **a)** The field of stationary capillary waves excited on the base of a water jet impinging on a horizontal water reservoir. **b)** The fluid pipe generated by a falling water jet impinging on a contaminated water reservoir. The field of stationary capillary waves is excited above the fluid pipe. The grids at right are millimetric.

the governing system parameters. We assume that, once the jet enters the fluid pipe, a boundary layer develops on its outer wall owing to the no-slip boundary condition appropriate there.

Balancing viscous and Marangoni stresses on the fluid pipe surface yields

$$\rho \nu \frac{V}{\delta_H} \sim \frac{\Delta \sigma}{H} \quad , \tag{11.35}$$

where $\Delta\sigma$ is the surface tension differential between the jet and reservoir, V is the jet speed at the top of the fluid pipe, and δ_H is the boundary layer thickness at the base of the fluid pipe. We assume that the boundary layer thickness increases with distance z from the inlet according to classical boundary layer scaling:

$$\frac{\delta}{a} \sim \left(\frac{\nu z}{a^2 V}\right)^{1/2} \quad . \tag{11.36}$$

Thus, at the base of a pipe of height H

$$\delta(H) = \left(\frac{\nu H}{a^2 V}\right)^{1/2} \tag{11.37}$$

Substituting for $\delta(H)$ from (11.36) into (11.35) yields

$$H \sim \frac{(\Delta \sigma)^2}{\rho \mu V^3} \tag{11.38}$$

The pipe height increases with the surface tension differential, and decreases with fluid viscosity and jet speed.

357 Interfacial Phenomena
Fall 2010